Journal of Drug Delivery Science and Technology 55 (2020) 101402

Contents lists available at ScienceDirect

Journal of Drug Delivery Science and Technology

journal homepage: www.elsevier.com/locate/jddst

Synergistic anticancer effects of electrospun nanofiber-mediated codelivery of Curcumin and Chrysin: Possible application in prevention of breast cancer local recurrence

Sara Rasouli[a], Maryam Montazeri[b], Samira Mashayekhi[a], Shima Sadeghi-Soureh[a], Mehdi Dadashpour[c], Hanieh Mousazadeh[c], Abbas Nobakht[d], Nosratollah Zarghami[c], Younes Pilehvar-Soltanahmadi[a,*]

[a] Cellular and Molecular Research Center, Cellular and Molecular Medicine Institute, Urmia University of Medical Sciences, Urmia, Iran
[b] Department of Medical Biotechnology, Faculty of Advanced Sciences and Technology, Tehran Medical Sciences, Islamic Azad University, Tehran, Iran
[c] Hematology and Oncology Research Center, Tabriz University of Medical Sciences, Tabriz, Iran
[d] Research Institute for Fundamental Sciences (RIFS), University of Tabriz, Tabriz, Iran

ARTICLE INFO

Keywords:
Nanofiber
Curcumin
Chrysin
Breast cancer
Combination chemotherapy

ABSTRACT

To decrease the locoregional recurrence of breast cancer, the *in vitro* anticancer efficacy of electrospun nanofibers (NFs) co-loaded with Curcumin (Cur) and Chrysin (Chr), as natural anticancer compounds, against T47D breast cancer cells was evaluated. According to FE-SEM results, the randomly oriented bead-free CurChr co-loaded PLGA/PEG fibers presented more interconnection among the fibers with increased average diameter to around 800 nm. Also, co-loading Cur and Chr into the NFs improved mechanical properties than single drug-loaded NFs. The *in vitro* release profile indicated the almost identical and prolonged release profile of drugs from CurChr-NFs that were lower than that from Cur-NFs and Chr-NFs. Based on MTT, CurChr-loaded PLGA/PEG NFs displayed effectively synergistic antiproliferative activities than the single drug-loaded NFs. Among loading different non-constant ratios of Cur and Chr in polymeric NFs, 10:5% (wt:wt%) CurChr-NFs exhibited the best synergistic cytotoxicity against the cells and could further altered the mRNA levels of bax, bcl-2, p53, Cyclin D1, caspase-3, caspase-7, and hTERT genes. In conclusion, the dual drug-loaded NFs showed an excellent capacity to inhibit T47D breast cancer cells *in vitro* than the single drug-encapsulated NFs. Therefore, the fabricated dual drug-encapsulated NFs may achieve a safe and suitable application for breast cancer relapse rate after surgery.

1. Introduction

Local or regional recurrence of breast cancer happens in average 9% of cases within 5–10 years after lumpectomy [1]. Local breast cancer recurrence is due to remain a small group of cancer cells in the breast after primary tumor resection or de novo breast tumor formation [2]. So, there is a noticeable need to develop agents that effectively eradicate the residual tumor cells and hamper the local breast cancer relapse [3].

Chemotherapy and radiotherapy cause unwanted and severe adverse effects and a significant reduction in life quality. Furthermore, extremely high costs and toxicities of some therapies applying chemotherapeutic drugs restrict their effectiveness [4,5]. Hence, exploring efficient and safe chemotherapeutic agents with minimal side effects is crucial and phytochemicals are hopeful bioproducts for such therapeutic uses [6]. Numerous phytochemicals have been developed and applied in clinical practice due to their strong anticancer effects, such as camptothecin, vincristine and paclitaxel [7]. Polyphenols especially Curcumin (Cur) and Chrysin (Chr) are the most important natural anticancer compounds, which have received immense interest in the past two decades owing to their proven safety and efficacy [8,9].

Cur, an bioactive ingredient from spice turmeric, has been found to possess anticancer and chemoprevention effects on numerous types of cancer especially breast cancer [10,11]. several *in vitro* and *in vivo* findings have been revealed that Cur exerts anticancer effects via a network of intricate molecular signaling mechanisms, involving proliferation, human epidermal growth factor receptor 2 (HER2) and estrogen receptor (ER) pathways. Also, experimental evidence has revealed that Cur regulates the genes involved in cellular growth and dead in breast cancer cells [12].

* Corresponding author.
E-mail address: ypilehvar@umsu.ac.ir (Y. Pilehvar-Soltanahmadi).

https://doi.org/10.1016/j.jddst.2019.101402
Received 21 May 2019; Received in revised form 31 October 2019; Accepted 18 November 2019
Available online 18 November 2019
1773-2247/

Chr, a natural flavone, widely found in several herbal extracts such as passion flowers, *Oroxylum indicum,* propolis and honey [13]. Cancer chemoprevention effect is the most promising among the numerous pharmacological activities presented by Chr [14,15]. Pre-clinical studies have revealed that Chr exhibits its antitumor activities via selective modulation of various cell signaling mechanisms that are connected to survival, proliferation, inflammation, angiogenesis, and metastasis of cancer cells. This wide range of anticancer effects in association with low toxicities and adverse side-effects to normal cells highlights a translational route for cancer treatment [16,17].

Despite the confirmed efficiency of Cur and Chr in breast cancer therapy, there are some main challenges restricting their clinical utilizes. Some factors restrict the use of free Cur and Chr for breast cancer therapy including poor water solubility, poor cellular uptake, low physicochemical stability, and rapid metabolism [18,19]. Numerous nanotechnological approaches have been employed to enhance the bioavailability and efficiency of the hydrophobic drugs [20–22].

In recent years, electrospun nanofibers (NFs) have acquired high attention for anticancer drug delivery because of their characteristic features such as high surface area to volume ratio, highly interconnected porous architecture, tailorable material properties, and also ease of drug incorporation into NFs during electrospinning [23,24]. The architecture and porosity of NFs can influence the release of drug from these NFs [25]. Also, the medicated NFs can be simply fix to the targeted region through regulating their shape and size [26]. Therefore, the drug-encapsulated NFs have been assumed to have a hopeful use on preventing local cancer recurrence after resection. Poly (lactic-co-glycolic acid)/poly (ethylene glycol) (PLGA/PEG) has been extensively employed to manufacture NFs with drug delivery abilities due to its superior biocompatibility and biodegradability [27].

In the field of cancer therapy, the application of a single drug is uncommon due to the toxicity of high doses, the heterogeneity of cancer cells, and their drug resistance [26]. The combination treatment is a promising approach to enhance the therapeutic efficiency and reduce the side effects [28]. However, it is difficult to achieve ideal antitumor effects through combination of free drugs because of their serious toxic side effects in human bodies, and diverse pharmacological activities and pharmacokinetic [29]. Hence, co-delivery approach including two or more various therapeutic agent has been suggested to reduce the dose of drugs and to obtain synergistic therapeutic effects in treating cancer. Several multidrug delivery systems including nanoparticles, liposomes, NFs, polymer–drug conjugates, and micelles have been designed for co-delivery of Cur and Chr with other anticancer agents and reported to exhibit significant anticancer activities [30]. However, there are no reports on application of electrospun NF-based implantable systems for localized co-delivery of Cur and Chr against breast cancer cells. The aim of the present study is to fabricate a dual drug delivery system based on polymeric electrospun NFs for co-releasing of two natural anticancer agents, Cur and Chr, and evaluate their combinatorial/synergistic anticancer effects against T47D breast cancer cells.

2. Materials and methods

2.1. Fabrication of drug-loaded electrospun NFs

First, PLGA/PEG copolymers were synthesized through ring-opening polymerization procedure based on our previous works [31,32]. For fabrication of drug-loaded electrospun NFs, PLGA/PEG copolymers were dissolved in DCM: Methanol at a ratio of 4:1 (*v/v*) to prepare a 10% *w/v* solution. Gel permeation chromatography (GPC; 10A series, Shimadzu, Japan) was used to determine the number of molecular weight (Mn) and polydispersity index (PDI) of the copolymer.

To obtain drug-loaded PLGA/PEG solutions, different weight ratios of Cur and Chr (5:0, 10:0, 0:5, 0:10, 5:10, 5:5 and 10:5 wt:wt%, respectively, with respect to the PLGA/PEG content) were added to PLGA/PEG solution and stirred magnetically for 8 h at 25 °C. The obtained solutions were fed in a 5 mL plastic syringe with a blunted 22-gauge needle, and the flow rate of solution maintained at 2 ml/h. The electrospun NFs were collected by a foil-coated rotating collector. The electrospinning was carried out at a range of 22–25 kV and needle-to-collector distance of 200 mm. The gained NFs were dried for 24 h under vacuum oven to remove the residual solvent. Inductively coupled plasma mass spectrometry (ICP-MS) and high performance liquid chromatography (HPLC), respectively, were used to determine the drug contents in the NFs. The encapsulation efficiency was measured as the following equation:

$$\text{Encapsulation Efficiency}(\%) = \frac{\text{weight of the drug in nanofibers}}{\text{weight of the feeding drugs}} \times 100$$

2.2. Characterization of drug-loaded electrospun NFs

The surface morphology of the electrospun NFs was studied by field emission scanning electron microscopy (FE-SEM) (MIRA3 TESCAN, Czech) at an accelerating voltage of 25 KV. The average diameter of the NFs was calculated from the FE-SEM photographs using image analysis software (Image J, National Institutes of Health, Bethesda, VA).

The chemical configuration of electrospun NFs were investigated through a Fourier transform infrared (FTIR) Spectrophotometer (IRPrestige-21; Shimadzu, Kyoto, Japan).

The NFs were cut into rectangular strips of 10 mm × 50 mm, and were tested for their mechanical properties using a Universal Testing Machine (1446, Zwick, Germany) with 10 N of load cell and 10 mm/min of crosshead speed.

2.3. In vitro drug release

To detect the release pattern of drugs from the drug-encapsulated NFs, NFs were cut into 20 mm × 20 mm square pieces and their weight were calculated. All the NFs were placed in a tube filled with 10 mL PBS: ethanol (70:30), pH 7.4, and shaken with the speed of 100 rpm in a shaker with temperature 37 °C. At preselected time intervals, 3 ml of the release medium was removed and replaced with an equal volume of fresh PBS. The amounts of the released Cur and Chr in the reserved samples were measured using a calibration curve at the wavelength where Cur and Chr exhibited their maximum absorbance (427 and 348 nm, respectively), quantitatively monitored using UV–visible spectrophotometer (Shimadzu, Tokyo, Japan). Therefore, the accumulative ratios of the discharged Cur and Chr were considered as a function of time.

2.4. In vitro cytotoxicity

The cytotoxic effects of drug-encapsulated NFs on T47D cells were evaluated by MTT assay. First, The NFs were washed thrice with 70% ethanol, and then sterilized under UV light for 30 min. Then, T47D cells were inoculated to each well of 48-well plates at a density of 8×10^3 cells in RPMI 1640 medium, containing 10% FBS, and grown for 24 h. After that, the cells were treated in triplicate manner with drug-loaded PLGA/PEG NFs and incubated at 37 °C in 5% CO_2 for 72 h. At the end of this period, medium was removed and 100 μL of MTT solution was added to each well and incubated for 4 h. Then, the medium was removed, 200 μL of DMSO was added to dissolve the formazan crystals, and the plates were shaken for 15 min. Finally, 200 μL of each sample was added to each well of 96-well plate to measure absorbance at 570 nm using ELISA reader (Dynex MRX).

2.5. Cell morphology analysis

T47D cells were seeded over glass coverslips coated with drug-loaded PLGA/PEG NFs. The treated T47D cells for 72 h were washed twice in PBS and fixed for 10 min with 2% glutaraldehyde followed by 20, 40, 60, and 80% ethanol gradient fixation. The samples were air dried at 37 °C. The fixed cells were coated with gold using a sputter coater for analysis of cell membrane integrity under FE-SEM.

2.6. Quantitative real-time PCR

The *in vitro* effectiveness of drug-loaded PLGA/PEG NFs to alter the expression of apoptotic genes (bax, bcl-2, caspase-3, and caspase-7), Cyclin D1, p53, and hTERT were analyzed using real-time PCR. Total RNA of treated cells with drug-loaded PLGA/PEG NFs was extracted using Trizol reagent (Gibco, Invitrogen) after 72 h, and extracted RNA was quantified using NanoDrop 2000 spectrophotometer (Thermo Scientific, USA). Using the High Capacity cDNA Reverse Transcription Kit (Applied Biosystems, USA), complementary DNA (cDNA) was reverse-transcribed. Quantitative real-time PCR was performed on the cDNA samples using the genes and β-actin primers and SYBR Green I Master Mix (Invitrogen SYBR GreenERTM qPCR SuperMix Universal, Invitrogen, Carlsbad, CA) in a Rotor gene 6000 system (Corbett, Qiagen, Australia). The housekeeping β-actin gene was used as the internal control. The Quantitative real-time PCR data were analyzed using double delta CT (ΔΔCT) method.

2.7. Statistical analysis

All experiments were carried out in triplicate independent tests. Findings were expressed as the mean ± SD. Data was analyzed using the software GraphPad Prism 7.01. Statistically differences between groups was determined using one-way ANOVA test. A value of $P < 0.05$ was considered as statistically significant.

3. Results and discussion

3.1. Size and morphological characterization

One the of common techniques to load drug into electrospun NFs is simultaneous encapsulation [33]. In this research, PLGA/PEG copolymers were applied to encapsulating Cur and Chr. PLGA is a semi-crystalline polymer well-known for its non-immunogenicity, good compatibility, and biodegradability *in vivo* on the cell biology [34]. Because of non-toxic nature and flexible mechanical properties, PLGA is appropriate polymer for biomedical applications. Copolymerization of PLGA with PEG, a kind of natural material with excellent biocompatibility and low cytotoxicity, can improve hydrophilicity and biodegradability of both polymer, and therefore they may find many applications [35].

GPC method was used to determine the molecular weight of copolymer. The Number-average molecular weight (Mn) and Weight-average molecular weight (Mw) of PLGA-PEG-PLGA were 7865 and 9542, respectively. The Polydispersity (PDI = Mw/Mn) of copolymer was about 1.197, which presented a symmetric peak and had a relative narrow molecular weight. In this study, it was used a mixture of DCM and methanol as the spinning solution. Cur and Chr were easily dissolved in PLGA/PEG/DCM/Methanol and a stable and homogeneous solution was attained. It has been showed which the lipophilic drugs such as Cur and Chr through hydrophobic binding interact with the hydrophobic polymer. Therefore, when the solution jet was quickly extended and the solvent vaporized, the drugs remained binding with PLGA/PEG, and thus acts as trap between polymeric chains. As shown in FE-SEM images (Fig. 1), the neat PLGA/PEG, Cur-loaded PLGA/PEG, Chr-loaded PLGA/PEG and CurChr-encapsulated PLGA/PEG fibers were randomly oriented to form smooth surface and bead-free *fi*brous structures under the optimized electrospinning conditions (an applied voltage 20 kV, tip-to-target distance of 20 cm and a 22-gauge blunt tip needle). For PLGA/PEG electrospun NFs, the dual drug-encapsulated NFs indicated more interconnection among the NFs while the single drug-loaded NFs indicated slight interconnections. The co-addition of Cur and Chr seems that could supply the connection of two NFs at the points where they were crossing with each other.

The diameter distributions of the neat PLGA/PEG and drug-loaded NFs were relatively narrow and found to be 400–500 nm in diameter, loading of 5 wt% and 10 wt% of Cur and Chr did not expressively change the diameter distribution of the NFs.

After the co-loading of Cur and Chr, the average fiber diameter was increased to around 800 nm. However, further increasing concentration of Cur and Chr to more than 15% was resulted in the formation of beads along the NFs and wither *fi*ber diameter distribution.

3.2. FTIR characterization

FTIR was carried out to show the chemical configuration of PLGA/PEG NFs and drug-encapsulated PLGA/PEG NFs (Fig. 2A). In Cur-PLGA/PEG NFs, a wider shift at 3300-3600 cm^{-1} shows the stretching of –H bonded –OH groups when Cur loaded into PLGA/PEG representing potential enhancement of hydrogen boding. The bands in the regions of 1759 and 1094-1186 cm^{-1} associated to ester group (O–C═O) (C–O), C–O–C ether group, and C–C bonds of PLGA/PEG NFs. The observed bands at 1625, 1590, and 1513 cm^{-1} are attributed to carbonyl group (C═O) and aliphatic and aromatic ethylene C═C bounds of Cur, respectively. The detected shift at Cur characteristic bands is associated to possible interaction it with PLGA/PEG NFs. The absorption band around 1500-1400 cm^{-1} showed the –C-O elongation frequency of –OH groups in Cur and Cur-PLGA/PEG NFs [29]. For Chr, the FTIR spectra of Chr showed bands at 2631, 2710, and 2921 cm^{-1} for stretching in the = C–H and C–H. Also, C═O group vibrations coupled with absorption bands in the regions 1612, 1576, and 1450 cm^{-1} and the double band in the ɣ-benzopyrone ring in the region 1653 cm^{-1} associated to carbon vibration in benzene and ɣ-pyrone rings, can be detected [19]. The results displayed successfully integration and loading of Cur and Chr into PLGA/PEG NFs.

3.3. Mechanical properties

Fig. 2B displays the characteristic strain–stress curves of the neat PLGA-PEG and drug-loaded PLGA/PEG NFs. The mechanical properties of NFs such as the Young's modulus, tensile strength, and strain at break were summarized in Table 2. In comparison to the blank PLGA/PEG NFs, the breaking strength and elastic modulus of the Cur-NFs and Chr-NFs were improved, that may be due to the effective loading of Cur and Chr in the PLGA/PEG NFs and more interconnected network of the NFs (due to a higher number of bridges and crossings). Because of strong interaction between the drugs and PLGA/PEG, co-loading Cur and Chr into the PLGA/PEG NFs led to increase the breaking strength and Young's modulus compared to single-drug loaded NFs. These results suggest which the mechanical feature of NFs can be enhanced with the loading of Cur and Chr.

3.4. Encapsulation efficiency and In vitro drug release

The content of Cur and Chr in the CurChr-loaded NFs were analyzed by ICP-MS and HPLC, respectively. The results of the weight percent of drugs loaded in the NFs as well as their encapsulation efficiency have been shown in Table 1.

The *in vitro* release profile of Cur and Chr from the NFs was studied in a mimicked physiological condition (pH 7.4, 37 °C). According to these data, the *in vitro* release profile in Fig. 3 showed the almost identical, prolonged and sustained release profile of Cur and Chr from NFs for 5 and 7 days without burst release.

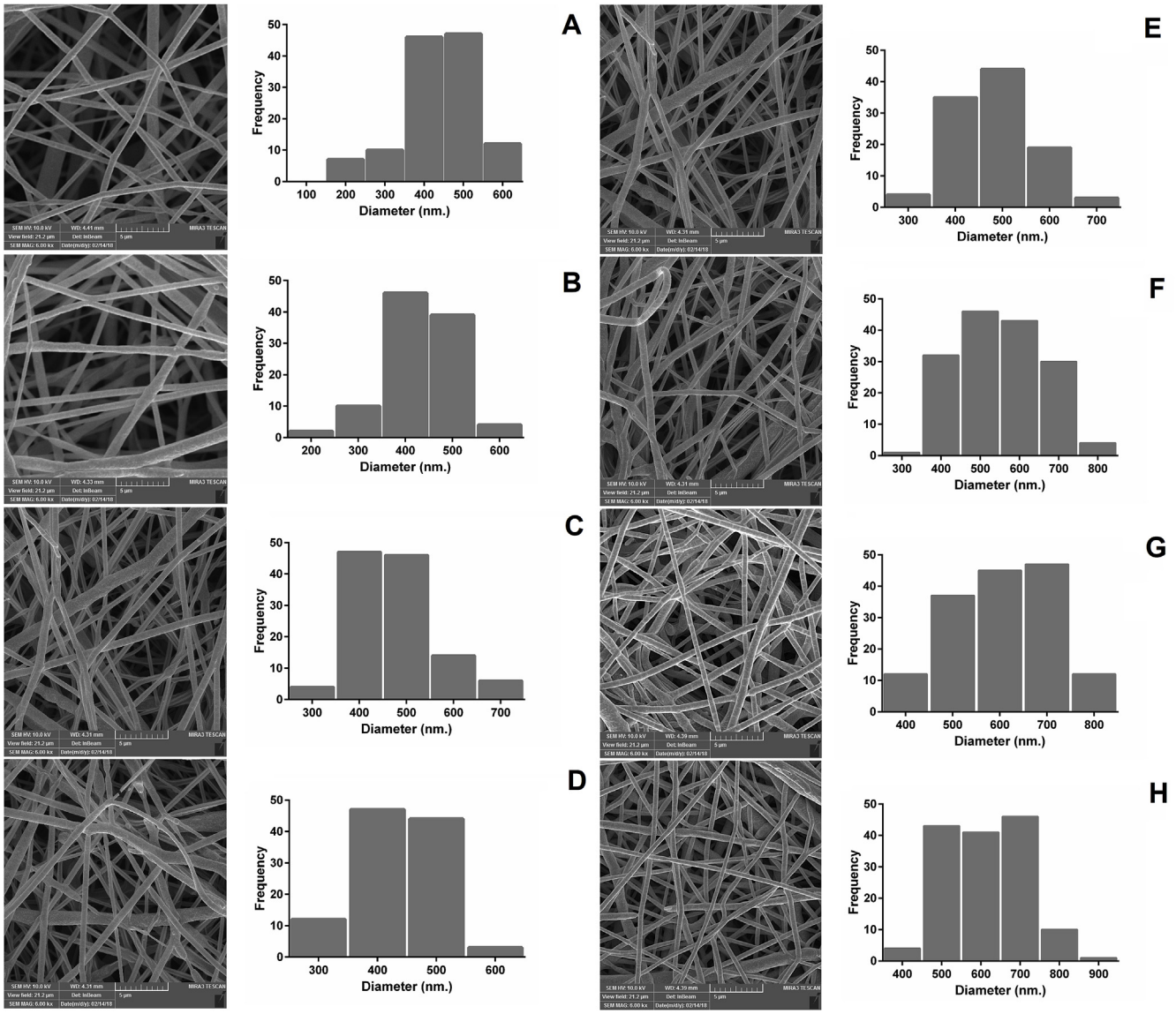

Fig. 1. FE-SEM images of nanofibers, A) PLGA/PEG, B) 5% Cur-PLGA/PEG, C) 10% Cur-PLGA/PEG, D) 5% Chr-PLGA/PEG, E) 10% Chr-PLGA/PEG, F) 5:5% CurChr-PLGA/PEG, G) 5:10% CurChr-PLGA/PEG, H) 10:5% CurChr-PLGA/PEG.

The absence of beads in the NFs enhances the surface area to volume ratio, better mechanical strength as well as the drug compatibility with the polymer/solvent electrospinning solution while the prolonged release profile confirmed the structural reliability of the NFs during the study.

Compared with that in 5% Cur-NFs (52.5%) and 10% Cur-NFs (55%) at 72 h, the drug release from CurChr-NFs at 5:10, 5:5, and 10:5 ratios were decreased to 37.5, 40.5, and 41.3%, respectively. Similarly, Chr release from CurChr-NFs at all three ratios was lower when compared with that from Chr-NFs. One possible explanation for this is that the more interactions among the drugs and PLGA/PEG in CurChr-NFs might cause further delaying in drug release.

During the 72 h, it was found that approximately 37.5, 40.5, and 41.3% of Cur and 48.5, 48, and 47.5% of Chr were released from the polymeric NFs with 5:10%, 5:5%, and 10:5% (wt:wt%) of Cur and Chr, respectively. In overall, the release rate of Chr within 72 h was faster than that of Cur from CurChr-NFs.

3.5. Cytotoxicity

The growth inhibitory effects of single drug-loaded NFs (5 and 10% Chr-NFs, and 5 and 10% Cur-NFs) and loaded NFs with different ratios of Cur and Chr (5:10, 5:5, and 10:5%, respectively), were studied against T47D breast cancer cells applying MTT assay after 72 h.

In the case of negative control and blank NFs (without drug loading), the samples did not display any cytotoxicity against the T47D breast cells up to 72 h. As shown in Fig. 4, all drug-loaded NFs inhibited the growth of breast cancer cells after 72 h incubation time, indicating that the drug-loaded PLGA/PEG NFs have ability to preserve the biological activity after high electric field.

Importantly, CurChr-loaded NFs displayed effectively higher cytotoxic effect against breast cancer cells in relative to the single drug-encapsulated NFs, that may be due to the corporative anticancer effects of the released Cur and Chr. Among loading different non-constant ratios of Cur and Chr in polymeric NFs, 10:5 (wt:wt%) CurChr–PLGA/PEG NFs exhibited the best cytotoxicity against T47D breast cancer cells. The gained findings indicated that the combined loading of Cur and Chr into PLGA/PEG NFs can improve the anticancer effects and might be suitable for postoperative therapy of breast tumors.

The exact nature of the interaction between Cur and Chr in combination forms was more investigated through the median-effect technique, where the Combination Index (CI) values higher than, equal to,

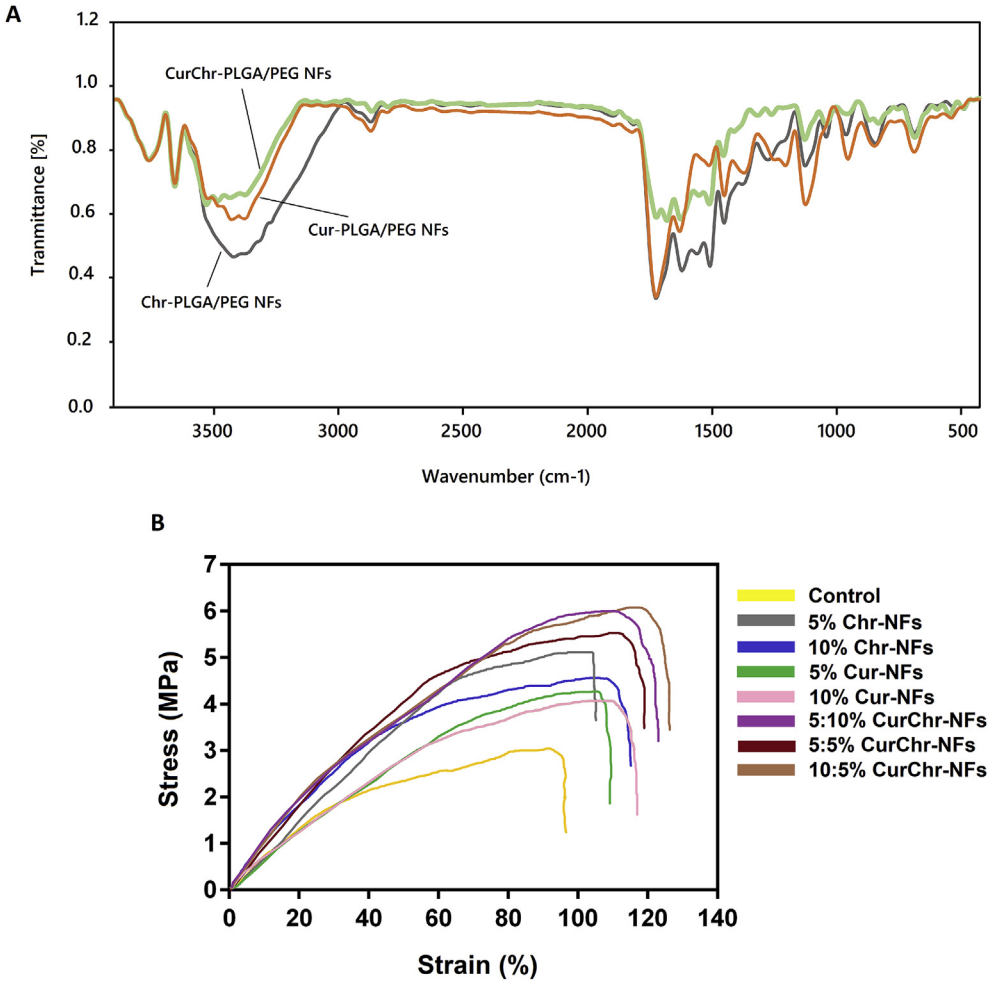

Fig. 2. FTIR results (A) and (B) typical stress–strain curves of the NFs.

or lower than 1 show antagonism, additivity, or, synergism in drug combinations, respectively [36].

Based on the combination index plot (Fig. 5), the CI values of 5:10, 5:5, and 10:5 (wt:wt%) CurChr-NFs were measured to be 0.94, 0.82, and 0.43, respectively, which verified that the combined loading of Cur and Chr into NFs presented synergistic inhibitory effects on the proliferation of T47D cells. It was found that 10:5% (wt:wt%) CurChr-NFs with smaller CI value displayed efficient synergistic growth inhibitory effect as compared with 5:10 and 5:5% CurChr-NFs and might induce greater cancer cell killing potency than single drug-loaded NFs.

3.6. FE-SEM of cell morphology analysis

The FE-SEM photographs of T47D cells seeded on neat PLGA/PEG NFs showed cell growth and proliferation while the cells seeded over drug-loaded PLGA/PEG NFs clearly showed distinctive morphology. The cells on neat PLGA/PEG NFs were able to grow properly by maintaining intact morphology and suitable cell junction. After 72 h of incubation time, the cells seeded on drug-loaded NFs showed alteration in the morphology typical of apoptotic cells such as formation of apoptotic bodies, plasma membrane blebbing, cell degeneration, and lysis. Fig. 6 shows the cell morphology on neat PLGA/PEG and CurChr-loaded PLGA/PEG NFs which demonstrates the induction of apoptosis in the cells treated with drug-loaded NFs whereas neat PLGA/PEG NFs support the proliferation and growth of T47D breast cancer cells.

3.7. Gene expression analysis

Apoptosis is a gene regulation occurrence, that is necessary equally for physiological and pathological conditions [37]. To confirm the stimulation of the apoptotic signaling pathways through drug-loaded NFs, the expression of different apoptotic genes (bax, bcl-2, caspase-3, and caspase-7), Cyclin D1, p53, and hTERT were quantitatively investigated through real-time PCR. The expression levels of all genes were normalized with the expression level of the house keeping gene β-actin.

Results showed that the mRNA expression levels of these genes were changed by single and combined drug-loaded NFs in relative to control (Fig. 7). While the mRNA levels of bax, caspase-3, and caspase-7 and

Table 1
The content of Cur and Chr in the CurChr-loaded NFs analyzed by ICP-MS and HPLC.

Drug-loaded NFs	Different weight (wt) ratios of Cur and Chr with respect to the polymer	wt% of Cur in wt% of polymers	wt% of Chr in wt% of polymers	EE% for Cur	EE% for Chr
CurChr-NFs	5:10 (wt:wt%)	4.1 ± 1.0%	8.8 ± 2.2%	82%	88%
CurChr-NFs	5:5 (wt:wt%)	4.0 ± 0.8%	3.9 ± 0.2%	80%	78%
CurChr-NFs	10:5 (wt:wt%)	9.2 ± 0.7%	4.0 ± 1.0%	92%	80%

Table 2
Tensile properties of the NFs.

Sample	Tensile strength (MPa)	Elongation at bread (%)	Young's modulus (MPa)
neat PLGA/PEG NFs	3.10 ± 0.42	90.25 ± 23.45	98.87 ± 48.39
5% Chr-loaded PLGA/PEG NFs	5.23 ± 1.12	105.30 ± 21.38	82.75 ± 43.32
10% Chr-loaded PLGA/PEG NFs	4.55 ± 0.25	109.25 ± 35.12	78.55 ± 45.10
5% Cur-loaded PLGA/PEG NFs	4.65 ± 1.00	107.52 ± 41.39	87.89 ± 45.20
10% Cur-loaded PLGA/PEG NFs	4.37 ± 0.24	110.42 ± 25.37	88.74 ± 45.47
5:10% CurChr-loaded PLGA/PEG NFs	6.01 ± 1.10	112.42 ± 23.25	110.72 ± 24.37
5:5% CurChr-loaded PLGA/PEG NFs	5.55 ± 1.13	113.25 ± 48.21	108.90 ± 39.23
10:5% CurChr-loaded PLGA/PEG NFs	6.12 ± 0.15	118.15 ± 12.20	114.92 ± 47.20

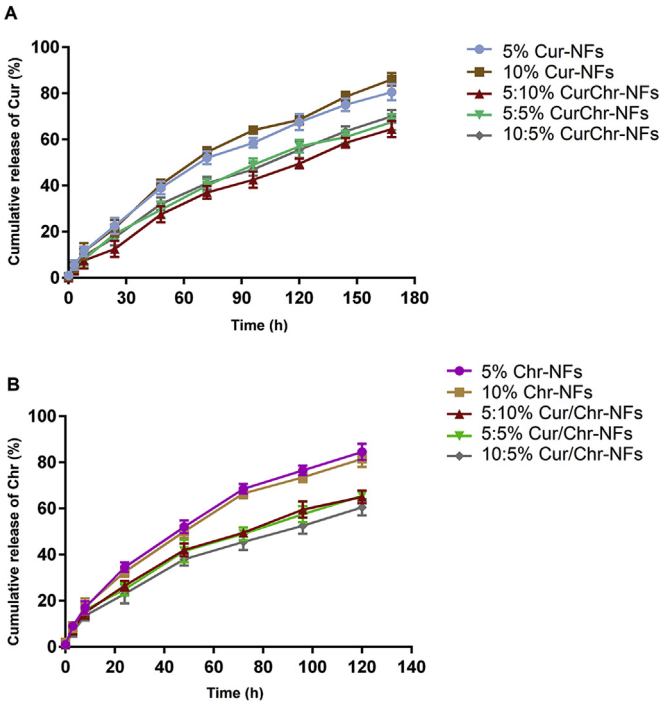

Fig. 3. Cumulative release profiles of (A) Cur and (B) Chr. results are expressed as the mean ± SEM (n = 3).

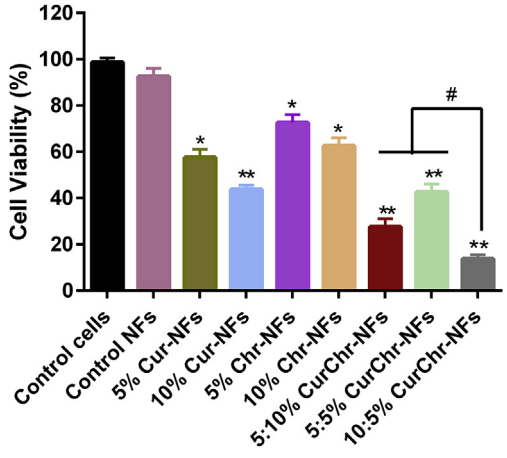

Fig. 4. *In vitro* cytotoxicity of the nanofibers to the T47D breast cancer cells after 72 h incubation. The data are presented as mean ± SD (n = 3).

also p53 were significantly up-regulated in the cells treated with the all drug-loaded NFs compared to control, CurChr-loaded NFs displayed effectively reduction in these genes than the single drug-loaded NFs. Among loading different non-constant ratios of Cur and Chr loaded into PLGA/PEG NFs, 10:5% (wt; wt%) CurChr-PLGA/PEG NFs could further

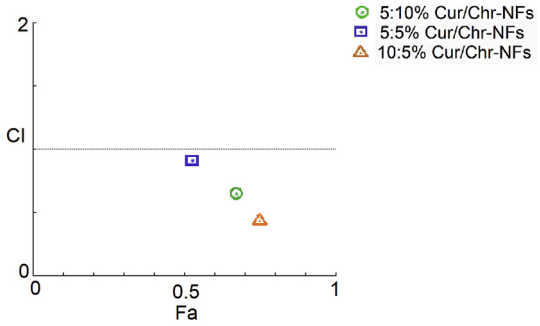

Fig. 5. Synergistic inhibitory effects of 5:5% CurChr-PLGA/PEG, 5:10% CurChr-PLGA/PEG, 10:5% CurChr-PLGA/PEG nanofibers against T47D breast cancer cells calculated through CompuSyn program and Chou-Talalay's Combination Index Theorem.

decline the mRNA levels of the genes. Also, it has been revealed that the mRNA levels of anti-apoptotic genes including cyclin D1, hTERT and bcl-2 significantly down-regulated in the cells treated with both single and dual drug-loaded NFs. As expected, dual drug-loaded NFs, specially 10:5% CurChr-PLGA/PEG NFs, showed further expression reduction of the genes at T47D cells seeded in relative to single drug-loaded NFs.

The process of apoptosis has a key function in cancer pathogenesis, and therefore the related genes are considered in investigations related to cancer initiation and progression [38]. Bax promotes apoptosis via inducing permeabilization in the mitochondrial outer membrane while Bcl-2 hinders cell dead through preventing Bax activity [39]. Both Bax and Bcl-2 have been reported to be transcriptional targets of tumor suppressor p53, which induces cell cycle arrest and/or apoptosis in response to a number of cellular stresses, including DNA damage, nucleotide deprivation and hypoxia. The malignant progression principally depends on the expression ratio of anti-apoptotic genes, such as BCL-2 and pro-apoptotic genes, such as BAX [40]. Besides, Caspase-3 and 7 are components of the cysteine protease family, which was known as main controller of apoptosis [41]. These enzymes are involved in the initiation stage and the end stage of apoptosis through chopping approximately 400 substrates [42].

The maintenance of telomere length is essential for prolonged cell proliferation, and ~85–90% of human cancers, including breast cancer, indicate high activity of telomerase. Three main subunits comprising telomerase complex included hTR (human telomerase RNA), TP1 (telomerase-associated protein 1), and hTERT (human telomerase reverse transcriptase) [43]. The hTERT gene is the most important regulator of telomerase activity. hTERT has high *expression* in all tissues, but in cancer cells usually have 5 fold-higher expression [44]. It was demonstrated that the inhibition of hTERT rapidly induces apoptosis in breast cancer cells [32]. Hence, targeting the hTERT in breast cancer may well be hopeful step in its treatment.

In this study, we demonstrated that co-delivery of two natural substances, Cur and Chr, through a polymeric electrospun nanofibrous scaffold exerts a synergistic anti-proliferative and pro-apoptotic effect on T47D breast cancer cells. However, studies on other types of breast

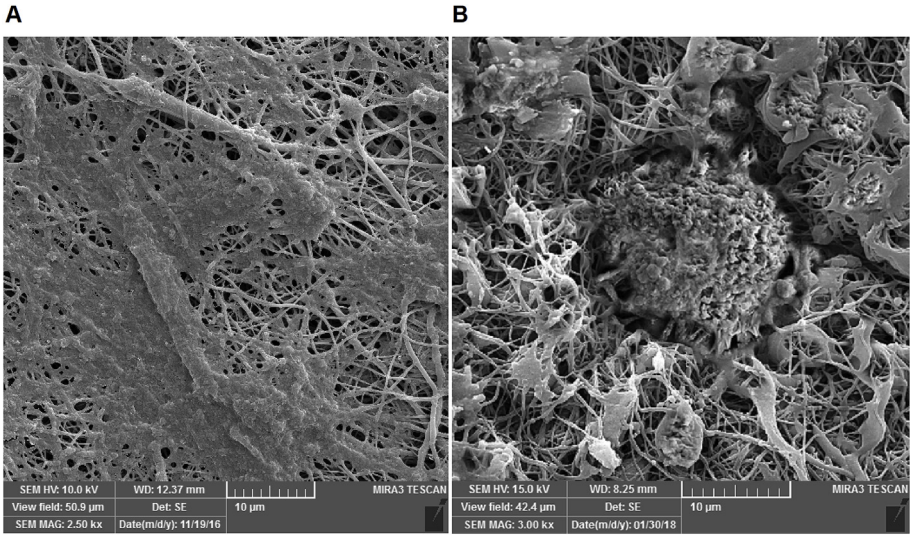

Fig. 6. FE-SEM images of T47D breast cancer cells seeded over neat PLGA/PEG NFs and CurChr-PLGA/PEG NFs for period of 72 h.

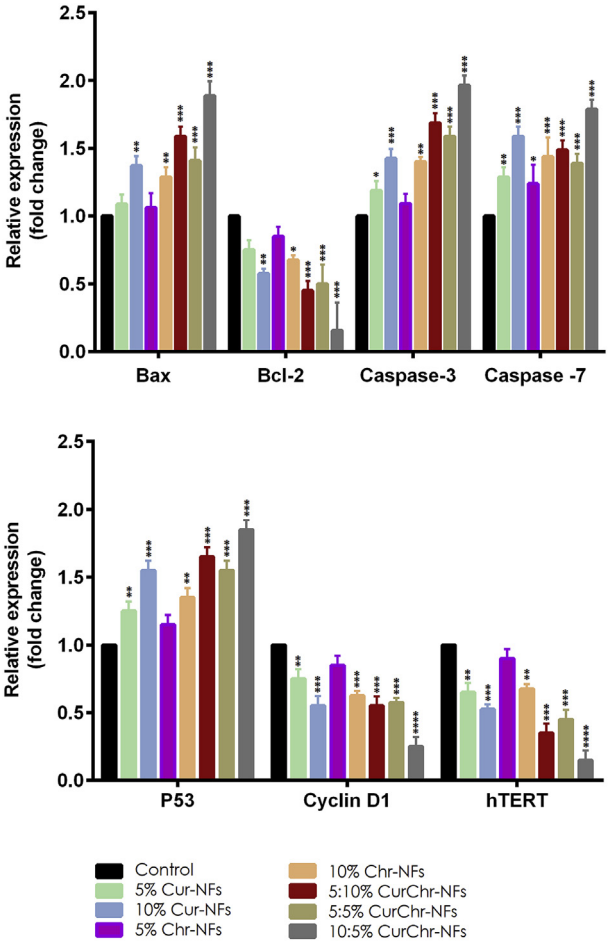

Fig. 7. The expression levels of Bax, Bcl-2, Caspase-3, Caspase-7, p53, Cyclin D1 and hTERT genes in relative to reference gene (GAPDH) T47D breast cancer cells treated with the nanofibers. $^{*}P < 0.05$, $^{**}P < 0.01$ and $^{***}P < 0.001$ vs. control was considered significant.

cancers, especially triple negative breast cancer cells, investigations on mechanism details of such approach, *in vivo* toxicity and efficiency studies are essential to more confirm the use of these implantable drug-encapsulated NFs for breast cancer treatment, which will be of our future interest.

4. Conclusions

In this study, a novel dual safe anticancer drug-encapsulated nanofibrous scaffolds was successfully prepared, that indicated a sustained dual drugs discharge profile and greater anticancer effects in compression with the single drug loaded nanofibrous scaffolds. The incorporation of Cur and Chr into the PLGA/PEG NFs can increase the mechanical property of the NFs, and decrease the initial burst discharge of the drug loaded in NFs, therefore raise the anticancer effects of the drugs. According to the preliminary findings at this work, applying electrospun NFs for co-delivery of natural anticancer compounds may provide a promising insight to open a novel therapeutic window for avoiding local recurrence of breast cancer after resection.

Declaration of competing interest

The authors declare that they have no competing interests.

Acknowledgments

The authors thank the Cellular and Molecular Research Center, Cellular and Molecular Medicine Institute, Urmia University of Medical Sciences for all support provided.

References

[1] H. Mellatyar, S. Talaei, Y. Pilehvar-Soltanahmadi, M. Dadashpour, A. Barzegar, A. Akbarzadeh, N. Zarghami, 17-DMAG-loaded nanofibrous scaffold for effective growth inhibition of lung cancer cells through targeting HSP90 gene expression, Biomed. Pharmacother. 105 (2018) 1026–1032.
[2] S. Talaei, H. Mellatyar, Y. Pilehvar-Soltanahmadi, A. Asadi, A. Akbarzadeh, N. Zarghami, 17-Allylamino-17-demethoxygeldanamycin loaded PCL/PEG nanofibrous scaffold for effective growth inhibition of T47D breast cancer cells, J. Drug Deliv. Sci. Technol. 49 (2019) 162–168.
[3] Q. Ding, Z. Li, Y. Yang, G. Guo, F. Luo, Z. Chen, Y. Yang, Z. Qian, S. Shi, Preparation and therapeutic application of docetaxel-loaded poly (d, l-lactide) nanofibers in preventing breast cancer recurrence, Drug Deliv. 23 (2016) 2677–2685.
[4] R. Kotecha, A. Takami, J.L. Espinoza, Dietary phytochemicals and cancer chemoprevention: a review of the clinical evidence, Oncotarget 7 (2016) 52517.
[5] S. Amirsaadat, Y. Pilehvar-Soltanahmadi, F. Zarghami, S. Alipour, Z. Ebrahimnezhad, N. Zarghami, Silibinin-loaded magnetic nanoparticles inhibit hTERT gene expression and proliferation of lung cancer cells, Artificial cells, nanomedicine, and biotechnology 45 (2017) 1649–1656.
[6] A. Alibakhshi, J. Ranjbari, Y. Pilehvar-Soltanahmadi, M. Nasiri, M. Mollazade, N. Zarghami, An update on phytochemicals in molecular target therapy of cancer: potential inhibitory effect on telomerase activity, Curr. Med. Chem. 23 (2016)

2380–2393.
[7] A. Chandra, Overview of cancer and medicinal herbs used for cancer therapy, Asian J. Pharm.: Free full text articles from Asian J Pharm 12 (2018).
[8] H. Fu, C. Wang, D. Yang, Z. Wei, J. Xu, Z. Hu, Y. Zhang, W. Wang, R. Yan, Q. Cai, Curcumin regulates proliferation, autophagy, and apoptosis in gastric cancer cells by affecting PI3K and P53 signaling, J. Cell. Physiol. 233 (2018) 4634–4642.
[9] M. Montazeri, Y. Pilehvar-Soltanahmadi, M. Mohaghegh, A. Panahi, S. Khodi, N. Zarghami, M. Sadeghizadeh, Antiproliferative and apoptotic effect of dendrosomal curcumin nanoformulation in P53 mutant and wide-type cancer cell lines, Anti Cancer Agents Med. Chem. 17 (2017) 662–673.
[10] C.D. Mock, B.C. Jordan, C. Selvam, Recent advances of curcumin and its analogues in breast cancer prevention and treatment, RSC Adv. 5 (2015) 75575–75588.
[11] H. Sadeghzadeh, Y. Pilehvar-Soltanahmadi, A. Akbarzadeh, H. Dariushnejad, F. Sanjarian, N. Zarghami, The effects of nanoencapsulated curcumin-Fe3O4 on proliferation and hTERT gene expression in lung cancer cells, Anti-Cancer Agents in Medicinal Chemistry, Formerly Current Medicinal Chemistry-Anti-Cancer Agents) 17 (2017) 1363–1373.
[12] S. Norouzi, M. Majeed, M. Pirro, D. Generali, A. Sahebkar, Curcumin as an Adjunct Therapy and microRNA Modulator in Breast Cancer, Current pharmaceutical design, 2017.
[13] A. Firouzi-Amandi, M. Dadashpour, M. Nouri, N. Zarghami, H. Serati-Nouri, D. Jafari-Gharabaghlou, B.H. Karzar, H. Mellatyar, L. Aghebati-Maleki, Z. Babaloo, Chrysin-nanoencapsulated PLGA-PEG for macrophage repolarization: possible application in tissue regeneration, Biomed. Pharmacother. 105 (2018) 773–780.
[14] E.R. Kasala, L.N. Bodduluru, C.C. Barua, R. Gogoi, Chrysin and its emerging role in cancer drug resistance, Chem. Biol. Interact. 236 (2015) 7–8.
[15] F. Mohammadian, Y. Pilehvar-Soltanahmadi, F. Zarghami, A. Akbarzadeh, N. Zarghami, Upregulation of miR-9 and Let-7a by nanoencapsulated chrysin in gastric cancer cells, Artificial cells, Nanomed. Biotechnol. 45 (2017) 1201–1206.
[16] Y. Deldar, F. Zarghami, Y. Pilehvar-Soltanahmadi, M. Dadashpour, N. Zarghami, Antioxidant effects of chrysin-loaded electrospun nanofibrous mats on proliferation and stemness preservation of human adipose-derived stem cells, Cell Tissue Bank. 18 (2017) 475–487.
[17] Z.J. Maasomi, Y.P. Soltanahmadi, M. Dadashpour, S. Alipour, S. Abolhasani, N. Zarghami, Synergistic anticancer effects of silibinin and chrysin in T47D breast cancer cells, Asian Pac. J. Cancer Prev. APJCP: Asian Pac. J. Cancer Prev. APJCP 18 (2017) 1283.
[18] P. Anand, H.B. Nair, B. Sung, A.B. Kunnumakkara, V.R. Yadav, R.R. Tekmal, B.B. Aggarwal, RETRACTED: Design of Curcumin-Loaded PLGA Nanoparticles Formulation with Enhanced Cellular Uptake, and Increased Bioactivity in Vitro and Superior Bioavailability in Vivo, Elsevier, 2010.
[19] Y. Deldar, Y. Pilehvar-Soltanahmadi, M. Dadashpour, S. Montazer Saheb, M. Rahmati-Yamchi, N. Zarghami, An in vitro examination of the antioxidant, cytoprotective and anti-inflammatory properties of chrysin-loaded nanofibrous mats for potential wound healing applications, Artificial cells, Nanomed. Biotechnol. 46 (2018) 706–716.
[20] R. Farajzadeh, N. Zarghami, H. Serati-Nouri, Z. Momeni-Javid, T. Farajzadeh, S. Jalilzadeh-Tabrizi, S. Sadeghi-Soureh, N. Naseri, Y. Pilehvar-Soltanahmadi, Macrophage repolarization using CD44-targeting hyaluronic acid–polylactide nanoparticles containing curcumin, Artificial cells, Nanomed. Biotechnol. 46 (2018) 2013–2021.
[21] F. Mohammadian, A. Abhari, H. Dariushnejad, A. Nikanfar, Y. Pilehvar-Soltanahmadi, N. Zarghami, Effects of chrysin-PLGA-PEG nanoparticles on proliferation and gene expression of miRNAs in gastric cancer cell line, Iran. J. Cancer Prev. 9 (4) (2016) e4190, https://doi.org/10.17795/ijcp-4190.
[22] M.M. Yallapu, P.K.B. Nagesh, M. Jaggi, S.C. Chauhan, Therapeutic applications of curcumin nanoformulations, AAPS J. 17 (2015) 1341–1356.
[23] M. Dadashpour, Y. Pilehvar-Soltanahmadi, S.A. Mohammadi, N. Zarghami, M. Pourhassan-Moghaddam, E. Alizadeh, M. Jafar Maleki, A. Firouzi-Amandi, M. Nouri, Watercress-based electrospun nanofibrous scaffolds enhance proliferation and stemness preservation of human adipose-derived stem cells, Artif Cells Nanomed. Biotechnol. 46 (4) (2018) 819–830.
[24] K. Nejati-Koshki, Y. Pilehvar-Soltanahmadi, E. Alizadeh, A. Ebrahimi-Kalan, Y. Mortazavi, N. Zarghami, Development of Emu oil-loaded PCL/collagen bioactive nanofibers for proliferation and stemness preservation of human adipose-derived stem cells: possible application in regenerative medicine, Drug Dev. Ind. Pharm. 43 (2017) 1978–1988.
[25] X. Li, M.A. Kanjwal, L. Lin, I.S. Chronakis, Electrospun polyvinyl-alcohol nanofibers as oral fast-dissolving delivery system of caffeine and riboflavin, Colloids Surfaces B Biointerfaces 103 (2013) 182–188.
[26] M. Chen, W. Feng, S. Lin, C. He, Y. Gao, H. Wang, Antitumor efficacy of a PLGA composite nanofiber embedded with doxorubicin@ MSNs and hydroxycamptothecin@ HANPs, RSC Adv. 4 (2014) 53344–53351.
[27] H.K. Makadia, S.J. Siegel, Poly lactic-co-glycolic acid (PLGA) as biodegradable controlled drug delivery carrier, Polymers 3 (2011) 1377–1397.
[28] D. Jafari-Gharabaghlou, Y. Pilehvar-Soltanahmadi, M. Dadashpour, A. Mota, S. Vafajouy-Jamshidi, L. Faramarzi, S. Rasouli, N. Zarghami, Combination of metformin and phenformin synergistically inhibits proliferation and hTERT expression in human breast cancer cells, Iranian journal of basic medical sciences 21 (2018) 1167.
[29] R. Farajzadeh, Y. Pilehvar-Soltanahmadi, M. Dadashpour, S. Javidfar, J. Lotfi-Attari, H. Sadeghzadeh, V. Shafiei-Irannejad, N. Zarghami, Nano-encapsulated metformin-curcumin in PLGA/PEG inhibits synergistically growth and hTERT gene expression in human breast cancer cells, Artificial cells, nanomedicine, and biotechnology 46 (2018) 917–925.
[30] J. Lotfi-Attari, Y. Pilehvar-Soltanahmadi, M. Dadashpour, S. Alipour, R. Farajzadeh, S. Javidfar, N. Zarghami, Co-delivery of curcumin and chrysin by polymeric nanoparticles inhibit synergistically growth and hTERT gene expression in human colorectal cancer cells, Nutr. Cancer 69 (2017) 1290–1299.
[31] Y. Pilehvar-Soltanahmadi, M. Nouri, MM. Martino, A. Fattahi, E. Alizadeh, M. Darabi, M. Rahmati-Yamchi, N. Zarghami, Cytoprotection, proliferation and epidermal differentiation of adipose tissue-derived stem cells on emu oil based electrospun nanofibrous mat, Exp. Cell Res. 357 (2017) 192–201.
[32] S. Javidfar, Y. Pilehvar-Soltanahmadi, R. Farajzadeh, J. Lotfi-Attari, V. Shafiei-Irannejad, M. Hashemi, N. Zarghami, The inhibitory effects of nano-encapsulated metformin on growth and hTERT expression in breast cancer cells, J. Drug Deliv. Sci. Technol. 43 (2018) 19–26.
[33] X. Hu, S. Liu, G. Zhou, Y. Huang, Z. Xie, X. Jing, Electrospinning of polymeric nanofibers for drug delivery applications, J. Control. Release 185 (2014) 12–21.
[34] E. Barcia, C. Herradón, R. Herrero-Vanrell, Biodegradable additives modulate ganciclovir release rate from PLGA microspheres destined to intraocular administration, Lett. Drug Des. Discov. 2 (2005) 148–149.
[35] K. Zhang, X. Tang, J. Zhang, W. Lu, X. Lin, Y. Zhang, B. Tian, H. Yang, H. He, PEG–PLGA copolymers: their structure and structure-influenced drug delivery applications, J. Control. Release 183 (2014) 77–86.
[36] M. Chatran, Y. Pilehvar-Soltanahmadi, M. Dadashpour, L. Faramarzi, S. Rasouli, D. Jafari-Gharabaghlou, N. Asbaghi, N. Zarghami, Synergistic anti-proliferative effects of metformin and silibinin combination on T47D breast cancer cells via hTERT and cyclin D1 inhibition, Drug Res. 68 (2018) 710–716.
[37] G.T. Williams, C.A. Smith, Molecular regulation of apoptosis: genetic controls on cell death, Cell 74 (1993) 777–779.
[38] M. Dadashpour, A. Firouzi-Amandi, M. Pourhassan-Moghaddam, M.J. Maleki, N. Soozangar, F. Jeddi, M. Nouri, N. Zarghami, Y. Pilehvar-Soltanahmadi, Biomimetic synthesis of silver nanoparticles using Matricaria chamomilla extract and their potential anticancer activity against human lung cancer cells, Mater. Sci. Eng. C 92 (2018) 902–912.
[39] I. Cavallari, G. Scattolin, M. Silic-Benussi, V. Raimondi, D.M. D'Agostino, V. Ciminale, Mitochondrial proteins coded by human tumor viruses, Front. Microbiol. 9 (2018) 81.
[40] J. Yu, L. Zhang, The transcriptional targets of p53 in apoptosis control, Biochem. Biophys. Res. Commun. 331 (2005) 851–858.
[41] N.A. Thornberry, The caspase family of cysteine proteases, Br. Med. Bull. 53 (1997) 478–490.
[42] A. Lüthi, S. Martin, The CASBAH: a searchable database of caspase substrates, Cell Death Differ. 14 (2007) 641.
[43] S. Pirmoradi, E. Fathi, R. Farahzadi, Y. Pilehvar-Soltanahmadi, N. Zarghami, Curcumin affects adipose tissue-derived mesenchymal stem cell aging through TERT gene expression, Drug Res. 68 (2018) 213–221.
[44] A. Zavari-Nematabad, M. Alizadeh-Ghodsi, H. Hamishehkar, E. Alipour, Y. Pilehvar-Soltanahmadi, N. Zarghami, Development of quantum-dot-encapsulated liposome-based optical nanobiosensor for detection of telomerase activity without target amplification, Anal. Bioanal. Chem. 409 (2017) 1301–1310.